MULTI-MODAL PIEZOELECTRIC CIRCUITS FOR VIBRATION SUPPRESSION OF A PLATE-LIKE WING UNDER ATMOSPHERIC TURBULENCE.

Tarcísio Marinelli Pereira Silva
Carlos De Marqui Junior
Department of Aeronautical Engineering, Engineering School of São Carlos – EESC, University of São Paulo, São Carlos, São Paulo, 13566-590, Brazil
tarcismarinelli@hotmail.com; demarqui@sc.usp.br

Abstract. This paper presents a numerical investigation on piezoelectric materials for suppressing atmospheric turbulence induced vibrations by and flutter. Traditional methods to attenuate these sources of vibrations consist of isolating springs, dampers or material design and they have the drawback of increasing weight. Piezoelectric transducers, on the other hand, are lighter (when compared to the traditional methods) smaller, and easily applied on most structures. The use of piezoelectric materials can be divided into active, passive, semi-passive and hybrid (active and passive simultaneously) according to the literature. In this work, the vibration suppression performance of these four techniques is investigated in several case studies. In all cases, two piezoeramic layers (bimorph in series) are embedded into the root of an elastic cantilever wing. The piezoaeroelastic model is obtained by combining an electromechanically coupled finite element model (based on Kirchhoff's assumptions) and an unsteady aerodynamic model. The turbulence model is based on Von-Karman's spectrum. The performance of each control strategy in a turbulent aerodynamic flow is investigated for airflow speeds ranging from low speeds to the flutter condition. The piezoaeroelastic behavior is analyzed in time and frequency domains.

Keywords: aeroelasticity, piezoelectric material, atmospheric turbulence and vibration control

1. INTRODUCTION

Atmospheric turbulence is a common, unavoidable and significant source of vibration. Flutter is a dynamic aeroelastic instability and its suppression is one of the main objectives of the research area of aeroelastic control. Flow induced vibrations is an important topic for modern aircraft, which use lightweight materials and structures. These aeroelastic vibrations lead to structural damage (with possible failure), undermine precision instruments, endanger human health and decrease flight performance and endurance. Here, the application of different piezoelectric circuits is discussed as an alternative to damp flow induced vibration.

In general, the main control techniques using piezoelectric materials are the passive and active ones. In active control applications, piezoelectric material is used as actuator (converse piezoelectric effect). An input voltage is applied to the piezoelectric material and mechanical strain is produced in order to reduce unwanted vibrations (Fuller and Elliot, 1996). Sensors and external source of energy are required. In passive case, the piezoelectric material is shunted to a passive electrical circuit where the mechanical energy converted to electrical energy (direct piezoelectric effect) is dissipated. The first applications from shunt damping literature are reported as a resistive circuit (Uchino and Ishii, 1988), the inductive shunt circuit (Forward, 1979), the resistive-inductive in series (Hagood and von Flotow, 1991) and the resistive-inductive in parallel (Wu, 1996).

The literature of aeroelastic control also presents piezoelectric based vibration control investigations. Heeg (1993) reports the use of piezoceramics as actuators for flutter suppression of a rigid wing mounted on a flexible system. The flutter speed of the wind tunnel device was increased by 20% when the control loop was closed. The control of dynamic aeroelastic phenomena was demonstrated in the Piezoelectric Aeroelastic Response Tailoring Investigation (PARTI) conducted at NASA Langley Transonic Tunnel (McGowan et al., 1998). A composite plate like wing with 36 piezoceramic patches was used and an increase of 12% in flutter dynamic pressure as well as 75% reduction of gust bending moment was achieved. Another widely known program is the Actively Controlled Response of Buffet Affected Tails (ACROBAT). Different authors investigate the use of piezoelectric actuators to damp tail buffeting of the F/A-18 aircraft (Moses, 1997; Moses, 1999; Hopkins et al., 1998; Durr et al., 1999). Giurgiutiu (2000) presents a comprehensive review of smart materials solutions for aeeroelastic control in fixed wings and helicopters.

Although the literature demonstrates the successful use of piezoelectric actuators in active aeroelastic control some issues have to be addressed: the large amount of power required, the added hardware as well as control law design and implementation (McGowan, 1999). An alternative approach is the use of passive control to damp a single mode or a number of modes (Fleming and Moheimani, 2005). In such case, an external source of energy is not required and simple electrical circuitry can be used. A few papers report the use of passive control schemes to damp aeroelastic oscillations. McGowan (1999) examines the performance of shunted piezoelectrics to reduce the aeroelastic response of a two-degree-of-freedom typical airfoil section. The numerical aeroelastic analysis shows that passive shunt damping circuits

ISSN 2176-5480

T.M.P. Silva and C. De Marqui Jr.
Multi-modal Piezoelectric Circuits for Vibration Suppression of a Plate-Like Wing Under Atmospheric Turbulence.

may provide a simple and effective method of subcritical aeroelastic oscillations control. Agneni et al. (2003) presents the modal-based modeling and analysis of the effectiveness of resistive-inductive shunted piezoelectric materials to damp aeroelastic systems. A weak performance of the passive controller in improving the stability margin (flutter envelope) of a composite wing of an unmanned glider is reported. However, the authors also report the weak ability of the passive devices to reduce the gust response amplitude of the wing in the neighborhood of flutter speed.

Since the frequencies of aeroelastic oscillations are very low (typically under 20Hz) the required inductances in passive control are extremely large and not practical. The synchronized switching damping (SSD) techniques (Richard et al., 1999, 2000; Clark, 2000; Guyomar et al., 2000; Corr and Clark, 2002) can address the issue of passive controllers (associated with large inductance required in aeroelastic cases) the complexities of active controllers. The SSD techniques are semi-passive methods that introduce the nonlinear treatment of the voltage output of the piezoelectric elements and induce an increase in mechanical to electrical energy conversion. In the semi-passive methods the piezoelectric material is kept in open circuit condition (maximum voltage output) except for a small period of time where voltage is canceled due to switch to small resistance (SSDS – synchronized switch damping on short-circuit) or inverted (SSDI – synchronized switch damping on inductor) due to brief switch to a resonant circuit. In both cases switching is performed synchronously with mechanical displacement. In the SSDS case, electrical energy is dissipated during voltage cancelation at short circuit condition resulting in increased damping effect. In the SSDI case, the required inductance is reduced if compared to the passive cases since it is related to electrical frequency and not related to mechanical oscillations.

The direct and the inverse piezoelectric effects can also be used simultaneously as presented in Zhao 2010. In the hybrid controllers, the mechanical energy converted to electrical energy is dissipated by the passive shunt-circuit, while the piezoelectric material simultaneously actuates on the base structure. This hybrid approach presents the advantage of affecting a wider frequency bandwidth than a purely passive control, and requires far less power supply than the purely active approach.

The piezoaeroelastic model in this work is obtained by combining an electromechanically coupled finite element (FE) model (De Marqui et al. 2009) with unsteady aerodynamic models (Doublet Lattice Method, Roger's approximation) and an atmospheric turbulence model. The turbulence is derived according to Wang and Frost (1980). The performance of different vibration control strategies (passive, semi-passive, active and hybrid) is verified at several flight conditions, ranging from low airflow speeds to the flutter condition. The generalized Hamilton's principle for electroelastic bodies is reviewed and the electromechanical finite element model is derived based on the Kirchhoff plate assumptions. The behavior of the piezoaeroelastic system is investigated in time and frequency domains.

2. PIEZOAEROELASTIC MODEL

The electromechanically coupled FE model of the piezoaeroelastic system shown in Fig. 1 is based on the Kirchhoff assumptions. The cantilevered plate-like wing presents piezoceramic layers perfectly bonded on the top and the bottom of the wing surface. The piezoceramic layers are poled in the thickness direction and covered by perfectly conductive electrodes with negligible thickness. The electrodes can be continuous (as in De Marqui et al. 2009) or segmented (as in De Marqui et al. 2010). De Marqui et al. 2009 detail the derivation of the electromechanically coupled FE model.
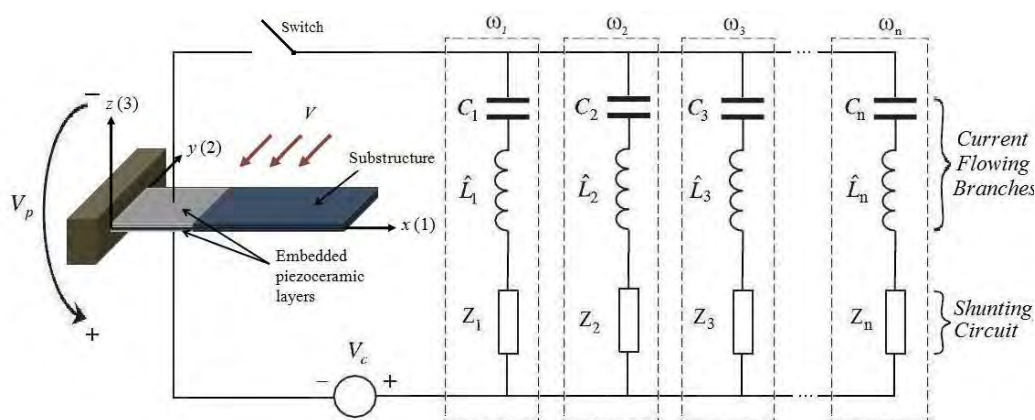
Figure 1: Piezoaeroelastic model.

Figure 1 also shows a multi-modal network connected to the piezoceramic layers for vibration control purpose. The purpose is to investigate vibration suppression performance of passive, semi-passive circuits, active and hybrid circuits. In Fig. 1, the series $\hat{C}_i - \hat{L}_i - Z_i$ is tuned to a specific resonance frequency ω_i of the system and the subscript n is the number of resonant frequencies to be considered. Z_i is the admittance of each passive circuit tuned to damp each

resonant frequency ω_i considered in the model. It is important to note that the n passive circuits Z_i are connected to a single pair of piezoceramics. Therefore, in order to avoid electrical interference among the n passive circuits Z_i, a series capacitive-inductive circuit (pass band filter, $\hat{C}_i$ and $\hat{L}_i$) is tuned to each resonant frequency ω_i. The filter appears to be in short circuit condition for ω_i and in open circuit condition for other frequencies (Behens et al. 2003,). V_c is the active control input. According to the setting of the multi-modal network in Fig. 1, different vibration controllers can be obtained. When $V_c = 0$ and the switch is permanently in short-circuit, a passive circuit is obtained. When the switch operates, a semi-passive control is obtained. When only the voltage source is considered in the circuit, an active control problem is investigated. When both the voltage source and passive admittances are considered (with the switch in permanently short-circuit condition), the hybrid network is obtained. The governing piezoaeroelastic equations for the elastic wing of Fig. 1 are

$$\bar{\mathbf{M}}\ddot{\mathbf{u}} + \bar{\mathbf{C}}\dot{\mathbf{u}} + \bar{\mathbf{K}}\mathbf{u} - \bar{\boldsymbol{\theta}}\mathbf{V_p} = q\bar{\mathbf{Q}}_{(\mathbf{k,M})}\mathbf{u} + q\bar{\mathbf{Q}}_{\mathbf{g(k,M)}}\frac{\mathbf{w_g}}{V} \tag{1}$$

$$\mathbf{C_p}\mathbf{V_p} + \mathbf{Q_p} + \bar{\boldsymbol{\theta}}^\mathbf{t}\mathbf{u} = \mathbf{0} \tag{2}$$

$$\mathbf{V_p} + \mathbf{V_c} = \hat{L}_1\ddot{\mathbf{Q}}_\mathbf{1} + Z_1\dot{\mathbf{Q}}_\mathbf{1} + \hat{C}_1^{-1}\mathbf{Q}_\mathbf{1}$$
$$\vdots$$
$$\mathbf{V_p} + \mathbf{V_c} = \hat{L}_N\ddot{\mathbf{Q}}_\mathbf{N} + Z_N\dot{\mathbf{Q}}_\mathbf{N} + \hat{C}_N^{-1}\mathbf{Q}_\mathbf{N} \tag{3}$$

$$\mathbf{Q_p} = \sum_{i=1}^{N}\mathbf{Q_i} \tag{4}$$

where $\bar{\mathbf{M}}$ is the modal mass matrix, $\bar{\mathbf{C}}$ is the modal damping matrix, $\bar{\mathbf{K}}$ is the modal stiffness matrix and $\bar{\boldsymbol{\theta}}$ is the modal electromechanical coupling matrix, q is the dynamic pressure, $\bar{\mathbf{Q}}_{(\mathbf{k,M})}$ is the matrix of generalizes aerodynamic forces (GAF) relative to the mean wind speed V, $\bar{\mathbf{Q}}_{\mathbf{g(k,M)}}$ is the GAF related to external atmospheric turbulence, V is the mean airflow speed, $\mathbf{w_g}$ is the turbulence vertical velocities vector, $\mathbf{u}$ is the modal vector of mechanical coordinates, $\mathbf{V_p}$ is the global vector of voltage outputs, $\mathbf{C_p}$ is the diagonal global capacitance matrix, $\mathbf{Q_p}$ is the global vector of electric charge outputs flowing in the piezoelectric patch. The subscripts 1 and N presented in Eq. 3 stand for the electrical parameter flowing in the series $\hat{C}_1 - \hat{L}_1 - Z_1$ and $\hat{C}_N - \hat{L}_N - Z_N$, respectively. In Eq. 1, the modal mechanical damping matrix is assumed to be proportional to the mass and stiffness matrices:

$$\bar{\mathbf{C}} = \alpha\bar{\mathbf{M}} + \beta\bar{\mathbf{K}} \tag{5}$$

where α and β are the constants of proportionality. It is noteworthy to mention that the aerodynamic term $\left(q\bar{\mathbf{Q}}_{(\mathbf{k,M})}\mathbf{u}\right)$ is an internal force that changes the piezoaeroelastic system behavior for each air speed considered, whilst the term $\left(q\bar{\mathbf{Q}}_{\mathbf{g(k,M)}}\frac{\mathbf{w_g}}{V}\right)$ is an external force. Both $\bar{\mathbf{Q}}_{(\mathbf{k,M})}$ and $\bar{\mathbf{Q}}_{\mathbf{g(k,M)}}$ are obtained from the Doublet Lattice Method (Albano and Rodden, 1969) (DLM) in frequency domain and can be projected in the time domain by using Roger's approximation (Roger, 1977). In the time domain representation additional states are added to the system.

3. TURBULENCE MODEL

Atmospheric turbulence is a continuous random process in which the time dependent variables exhibit irregular fluctuations. In practice, only statistical properties can be recognized and subjected to analysis. In this work, the stochastic turbulence signal ($\mathbf{w_g}$), describing the turbulence vertical velocities as function of time, has zero mean velocity and is calculated according to the following equation:

T.M.P. Silva and C. De Marqui Jr.
Multi-modal Piezoelectric Circuits for Vibration Suppression of a Plate-Like Wing Under Atmospheric Turbulence.

$$\mathbf{w}_{\mathbf{g}(\mathbf{f_r})} = \mathbf{g}_{\mathbf{a}(\mathbf{f_r})}\mathbf{\Phi}_{(\mathbf{f_r})} \tag{6}$$

where $\mathbf{g}_{\mathbf{a}(\mathbf{f_r})}$ is the stochastic random Gaussian noise in frequency domain, whose power spectrum is equal to the unity $\left(\left|\mathbf{g}_{\mathbf{a}(\mathbf{f_r})}\right|^2 = 1\right)$, and $\mathbf{\Phi}_{(\mathbf{f_r})}$ is the shaping filter derived from the Von-Karman spectrum. The Von-Karman spectrum is defined as shown in Eq. 7:

$$\left|\mathbf{\Phi}_{(\mathbf{f_r})}\right|^2 = \frac{2\sigma^2 L_g}{V}\frac{1+\frac{8}{3}\left(1{,}339\frac{L_g\mathbf{f_r}}{V}\right)^2}{\left(1+\left(1{,}339\frac{L_g\mathbf{f_r}}{V}\right)^2\right)^{\frac{11}{6}}} => \mathbf{\Phi}_{(\mathbf{f_r})} = \frac{0.0285\sigma\left(\frac{V}{L_g}\right)^{\frac{4}{3}}+0.3915\sigma\left(\frac{V}{L_g}\right)^{\frac{1}{3}}j\mathbf{f_r}}{\left(\frac{V}{1.339.2\pi L_g}+j\mathbf{f_r}\right)^{\frac{11}{6}}} \tag{7}$$

where $\left|\mathbf{\Phi}_{(\mathbf{f_r})}\right|^2$ is the Von-Karman spectrum, $\mathbf{\Phi}_{(\mathbf{f_r})}$ a solution for the Von-Karman spectrum, j is the imaginary number, $\mathbf{f_r}$ is the frequency in Hz, σ is the standard deviation and L_g the turbulence scale. The reader is referred to Wang and Frost (1980) for the derivation of the atmospheric turbulence model. The main use of power spectral density functions is to establish the frequency composition of the data which, in turn, bears an important relationship to the basic characteristics of a physical system exposed to interaction with the turbulence (Wang and Frost, 1980).

The Inverse Fast Fourier Transform (IFFT) of Eq. 6 yields the turbulence signal $\mathbf{w}_{\mathbf{g}(\mathbf{f_r})}$ in time domain. The turbulence signal in the time and frequency domain can be seen in Fig. 2a and Fig. 2b.
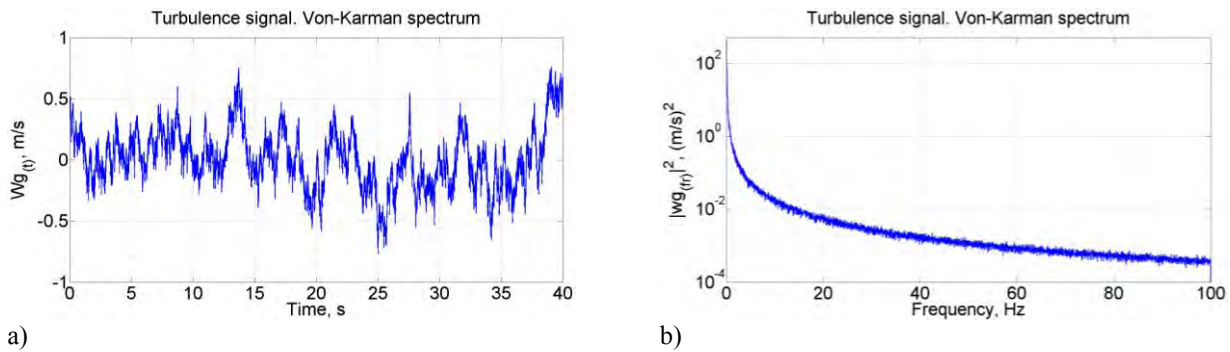
Figure 2: a) Turbulence vertical velocities vector in time domain. b) Turbulence vertical velocities vector in frequency domain

As shown in Fig. 2, atmospheric turbulence mainly excites low frequencies.

4. RESULTS

This section investigates the efficiency of the passive, semi-passive circuits as well as active and hybrid controllers to attenuate flutter oscillations and also atmospheric turbulence induced vibrations. In the first case study, the four vibration control techniques are investigated at the flutter speed and their performance presented in time and frequency domain. In addition, the capability of these four techniques to increase the flutter speed is investigated. In the second case, atmospheric turbulence is considered in the problem and the range of airflow speeds varies from almost zero to the flutter speed. Optimum load resistances (that give the maximum damping) were calculated for the passive and hybrid cases. For all circuits, the results are compared to the Short-Circuit (SC) and Open Circuit (OC) conditions.

In the two case studies, the aluminum cantilevered plate-like wing of Fig. 1 with two identical layers of PZT-5A embedded into the top and the bottom is used. The mass density of the piezoceramic layers is 7800kg/m^3 and they cover the entire wing chord from the wing root to 30% of the wingspan. Each piezoceramic layer has a thickness of 0.5 mm. The initial conditions are set to zero and the air density is assumed to be 1.225 kg/m^3. The mechanical properties of the elastic wing are given in tab. 1.

Table 1: mechanical properties of the sub-structure

Properties of the sub-structure: aluminum alloy Al 2024-T3	Value
Mass density of the sub-structure (Kg/m^3)	2750
Young's modulus of the sub-structure (GPa)	70.0
Span of the wing (mm)	1200
Chord of the wing (mm)	240
Thickness of the wing (mm)	3
Constant of proportionality: α	0.1635
Constant of proportionality: β	4.1711e-4

4.1 First Case Study

In this case, the effect of each control scheme considered in this work on the aeroelastic behavior of the wing is investigated. The flutter speed and the flutter frequency for the short circuit (SC) condition are 47.1 m/s and 7.75 Hz, respectively. In this case study, the aeroelastic behavior of the electromechanically coupled wing is investigated considering the passive controller (resistive-inductive in series - RLs), the SSDS and SSDI cases, a purely active controller and a hybrid controller (active and a resistive-inductive in series). The electrical outputs of these circuits are observed and compared. In typical flutter behavior, a coupling between bending and torsion modes is observed at the flutter speed. Therefore, a segmented electrodes configuration is assumed in the piezoceramic patches. As reported in the literature (De Marqui et al., 2010), segmented electrodes provide a better electrical output for pure torsion and bending-torsion coupled modes when compared to continuous electrodes.

Figure 3a and Fig. 3b show the piezoaeroelastic behavior of the system when a RLs passive circuit, a SSDS and a SSDI circuit are investigated. Flutter oscillations are suppressed when the different control schemes are used. However, one should note that the SSDI case has the best performance among the schemes considered in this work.
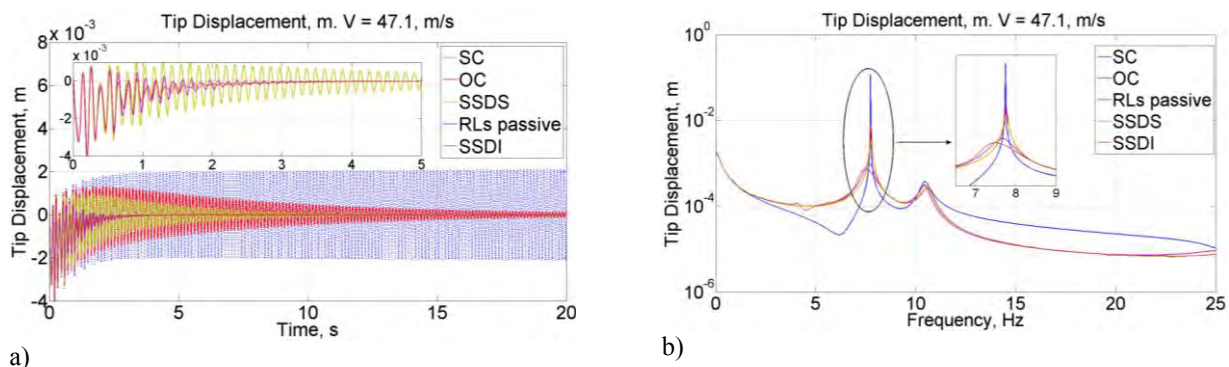
Figure 3: a) wing tip displacement in time domain. b) wing tip displacement in frequency domain.

The voltage and current outputs are shown in Fig 4a and Fig. 4b. One should note in Fig 4a the voltage inversion of the SSDI case and the voltage cancelation of the SSDS case.
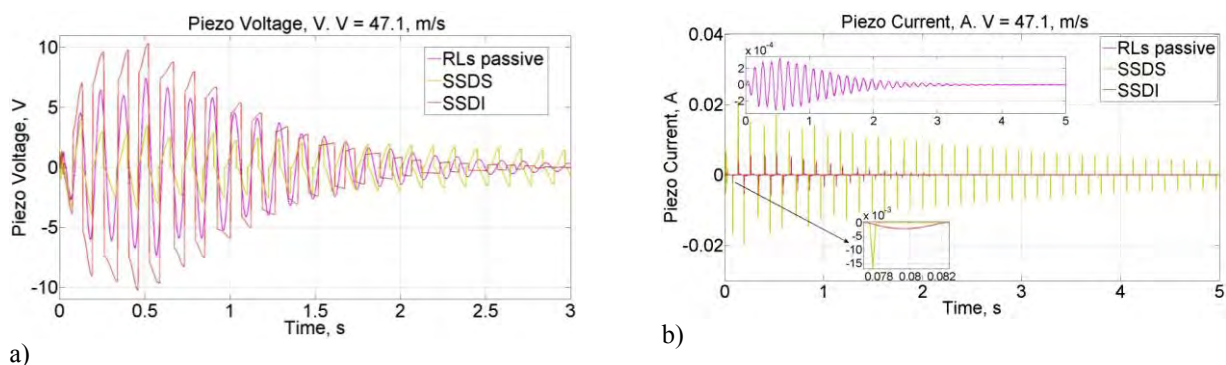
Figure 4: a) Voltage across the piezoceramic patch. b) Current across the piezoceramic patch.

The performance of the purely active and hybrid controllers are presented in Fig 5. The SSDI and the RLs passive circuits are also displayed for comparison with the active and hybrid controllers. The active controller and RLs hybrid controller have similar performances, and better than the SSDI case. In particular, the RLs hybrid case showed some

T.M.P. Silva and C. De Marqui Jr.
Multi-modal Piezoelectric Circuits for Vibration Suppression of a Plate-Like Wing Under Atmospheric Turbulence.

improvement when compared to the purely active control. However, it is important to note that the power consumed by the controllers (active and hybrid) is not negligible, as shown in the Fig. 6a and Fig. 6b.
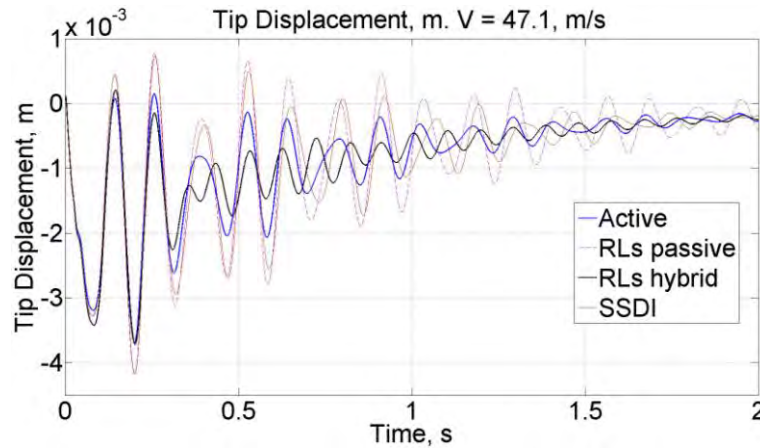
Figure 5: Piezoaeroelastic response when a purely active controller and a hybrid controller are used for flutter suppression**.**

a)

b)
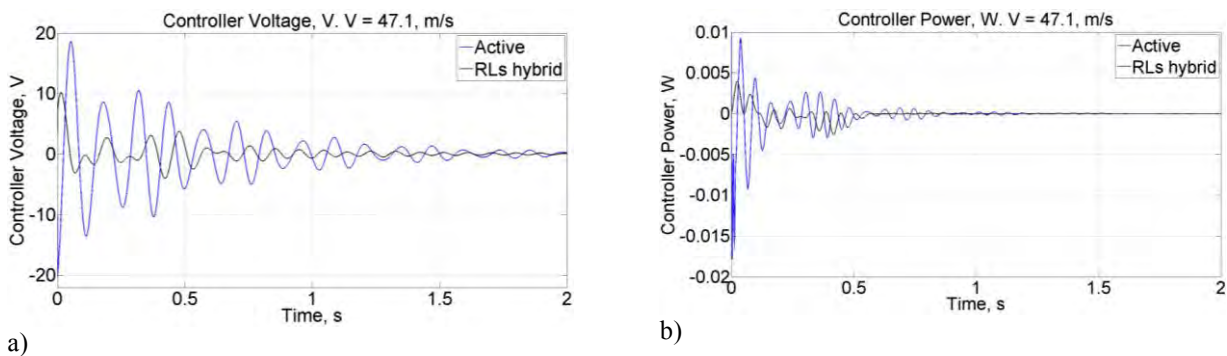
Figure 6: a) voltage applied by the voltage source. b) power required by the voltage source.

The voltage across the piezoceramic patch is equal to the inverse of the controller voltage for the purely active controller case. For the RLs hybrid case, the voltage across the piezoceramic is larger than the voltage in the active case as shown in Fig 7. Figure 7 also displays the RLs passive and the SSDI cases.
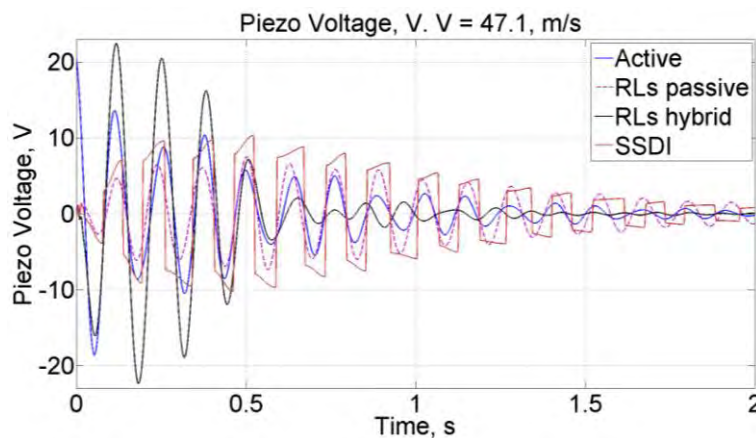
Figure 7: Voltage across the piezoceramic patch for different piezoelectric circuits.

Energy is continuously pumped into the structure from the surrounding fluid flow for airflow speeds larger than the flutter speed. The semi-passive SSDI circuit, the active and the hybrid controllers were investigated in the post flutter condition. Figures 8 show the flutter suppression when active and hybrid controllers are used. Although the oscillations

are not damped out when the SSDI scheme is used, the wing tip displacement is bounded and the wing presents acceptable mechanical amplitudes. It is important to remember that external energy is not required in the SSDI case, while power consumption of the active and hybrid cases is relatively large.
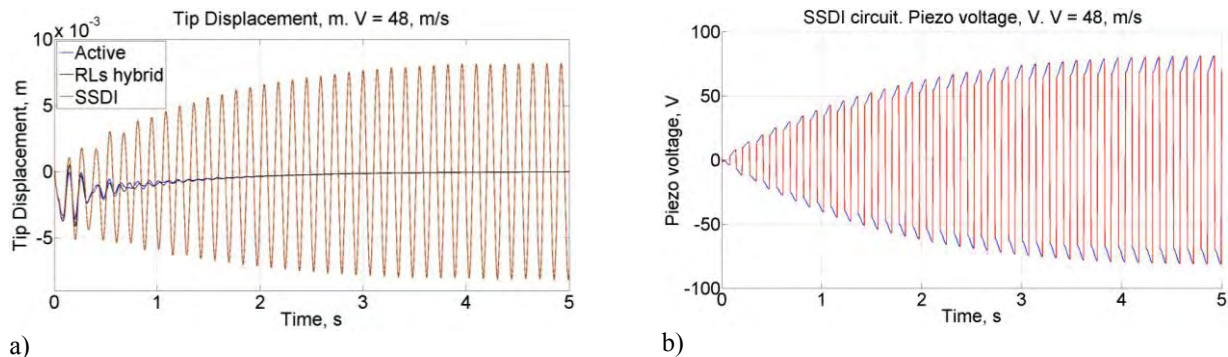
Figure 8: a) wing tip displacement under an after flutter airflow speed for different piezoelectric circuits. b) Voltage across the piezoceramic patch for the SSDI circuit.

Flutter was suppressed when the active and RLs hybrid controllers were used at airflow speeds larger than the flutter one. Although the active and the hybrid controllers suppress oscillations at the post flutter condition, the required energy increases with increasing airflow speed. In this work, the required controller voltage reaches 150V and the voltage across the piezoceramic patch exceeds 200V for the airflow speed of 53 m/s. It is important to note that voltages larger than 200V can depolarize the PZT 5A.

4.2 Second Case Study

In this second case study the performance of passive, semi-passive piezoelectric circuits, active controller and hybrid controllers for suppressing atmospheric turbulence induced vibrations is investigated with increasing airflow speed (1, 7.5, 25, 35 and 47.1 m/s). In this case study, it was observed that continuous electrodes are more convenient for vibration suppression when compared to the segmented scheme used in the previous case study. Atmospheric turbulence mainly excites low frequencies (Fig 2b), and the first resonant frequencies of the system studied here are related to bending modes. Figures 9a and 9b show the time and frequency domain responses of the aeroelastic system (with continuous electrodes) under atmospheric turbulence for the airflow speed of 1 m/s.
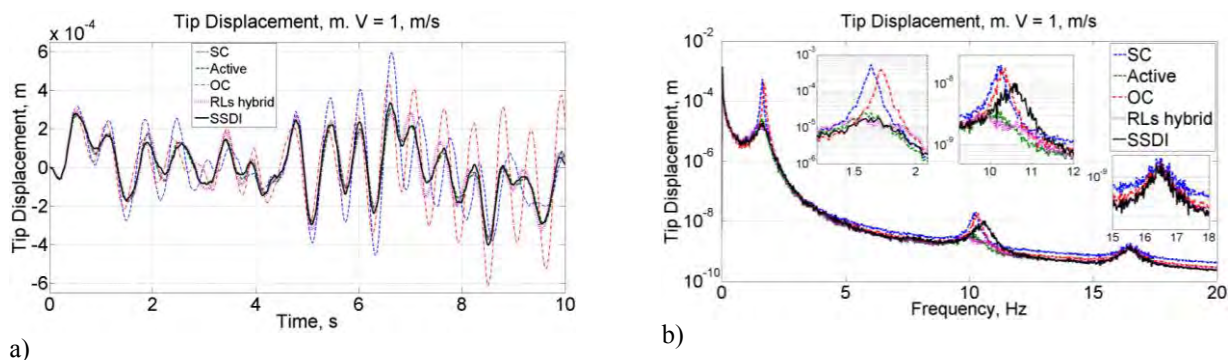
Figure 9: a) piezoaeroelastic response to an atmospheric turbulence in time domain. b) piezoaeroelastic response to an atmospheric turbulence in frequency domain.

As shown in Fig. 9a and the detailed view of Fig. 9b, considerable vibration reduction is achieved. In Fig. 9b, the multi-modal RLs hybrid circuit was set to damp the first three resonant frequencies (1.64Hz, 10.24Hz and 16.4Hz) while the SSDI circuit was adjusted for the first mode (1.64Hz). There is no effect on the first torsion mode (16.4Hz) since continuous electrodes are used in this case. In Fig. 9a, all circuits presented similar vibration attenuation.

Figure 10a and Fig 10b present the work performed by each controller for the case of Fig. 9. The work is the integral of the controller power signal: $W_c = \int |P_c| dt$. Figures 10a and 10b show that the active controller requires more energy (32%) than the RLs hybrid circuit to attenuate flow induced oscillations.

T.M.P. Silva and C. De Marqui Jr.
Multi-modal Piezoelectric Circuits for Vibration Suppression of a Plate-Like Wing Under Atmospheric Turbulence.

a)   b)
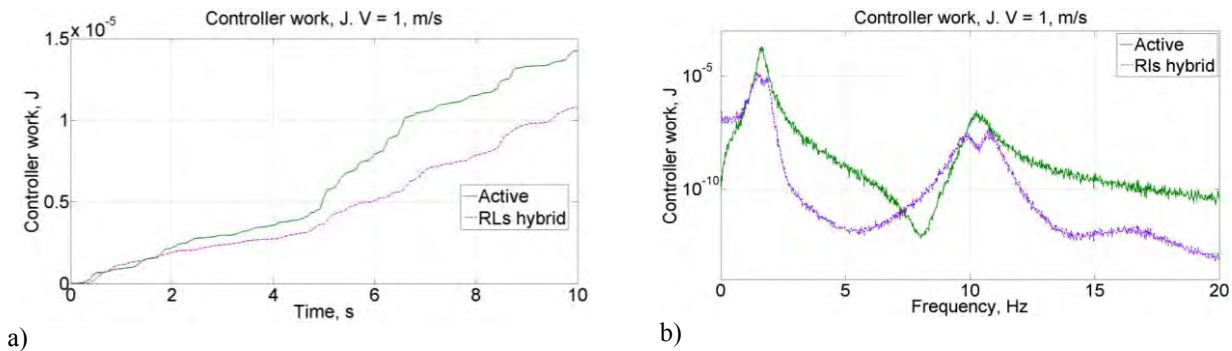
Figure 10: a) Energy required by the active and hybrid controller in time domain. b) Energy required by the active and hybrid controller in frequency domain.

Figure 11 shows the voltage across the piezoceramic patch and the tip for the SSDI case. One should note that switching is performed at the maximum tip displacement.
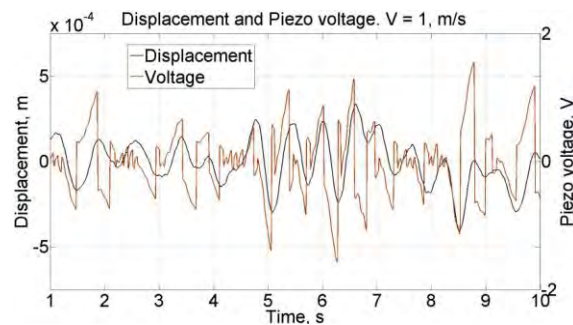
Figure 11: Voltage across the piezoceramic in comparison to the wing tip displacement for the SSDI circuit.

A simulation for the airflow speed of 7.5m/s is shown in Fig. 12a and Fig. 12b. Figures 12a and 12b show a similar behavior to Fig. 9a and 9b. The wing tip displacement is reduced when semi-passive circuit and the active and hybrid controllers are considered. In this case, the attenuation provided by the piezoelectric circuits is smaller than in Fig 9a and Fig. 9b. When the airflow speed of 1m/s is considered, less aerodynamic damping is present in the system. The effectiveness of the piezoelectric circuits to reduce vibration becomes less evident as the aerodynamic damping increases in the system.

a)   b)
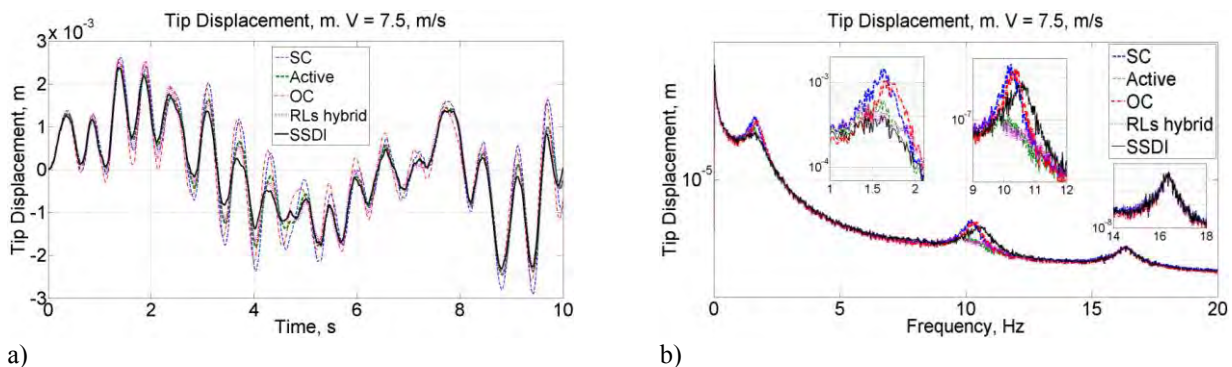
Figure 12: a) Piezoaeroelastic response to an atmospheric turbulence in time domain. b) Piezoaeroelastic response to an atmospheric turbulence in frequency domain.

Figures 13a and 13b show the power required by the active and hybrid controllers. The power required for the airflow speed of 7.5m/s is higher than the power required for the airflow speed of 1m/s (due to the larger aerodynamic loads and amplitudes). The power required by the controllers is related to the structure displacements and increases with increasing aerodynamic loads. In this case, the lower power consumption of the RLs circuit shows an interesting advantage over the purely active circuit. Although the performance of active and hybrid controllers is similar (in terms

of attenuation), the power required by the active side of the hybrid controller is smaller than the power required by the purely active controller.

a)   b)
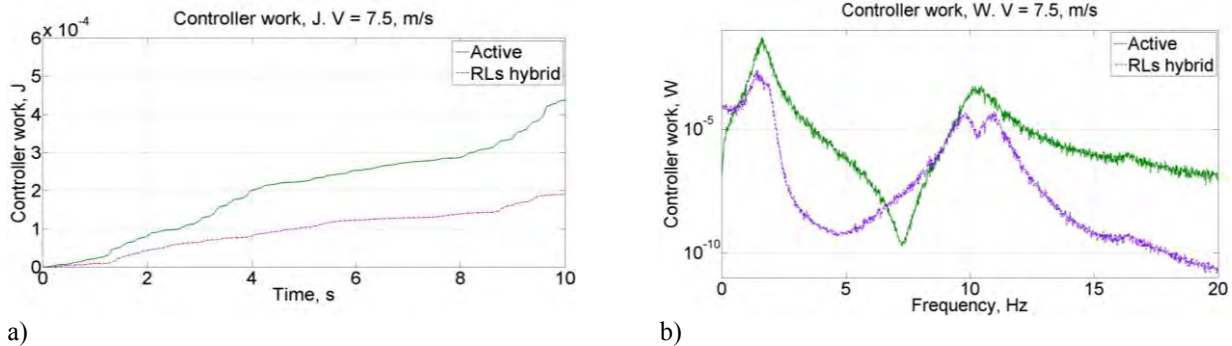
Figure 13: a) Energy required by the active and hybrid controller in time domain. b) Energy required by the active and hybrid controller in frequency domain

The voltage across the piezoceramic patch and the displacements for the SSDI case are presented in Fig. 14. As observed in Fig. 14, the switch operates at the maximum and minimum values of the wing displacements.
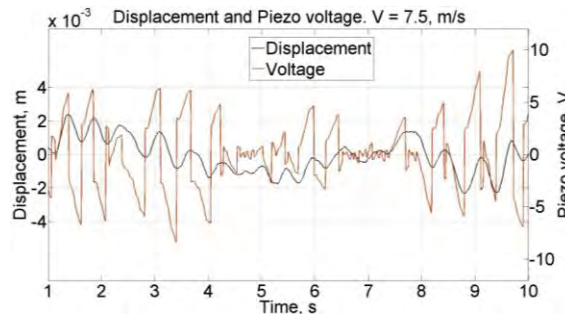
Figure 14: Voltage across the piezoceramic in comparison to the wing tip displacement for the SSDI circuit.

In the case of the elastic wing studied in this work, strong aerodynamic damping is present at 25m/s and the maximum aerodynamic damping is present at 35m/s. Figures 15a to 16b show the wing tip displacements in time and frequency domain for these two airflow speeds. As seen in Fig 15a to Fig. 16b, the effect of the piezoelectric circuits is no longer observable for airflow speeds of 25 m/s and 35 m/s. In frequency domain, no resonant peak is observed for the airflow speed of 25m/s and 35m/s due to the strong aerodynamic damping. This way, the performance of the different controllers cannot be discussed at these airflow speeds.

a)   b)
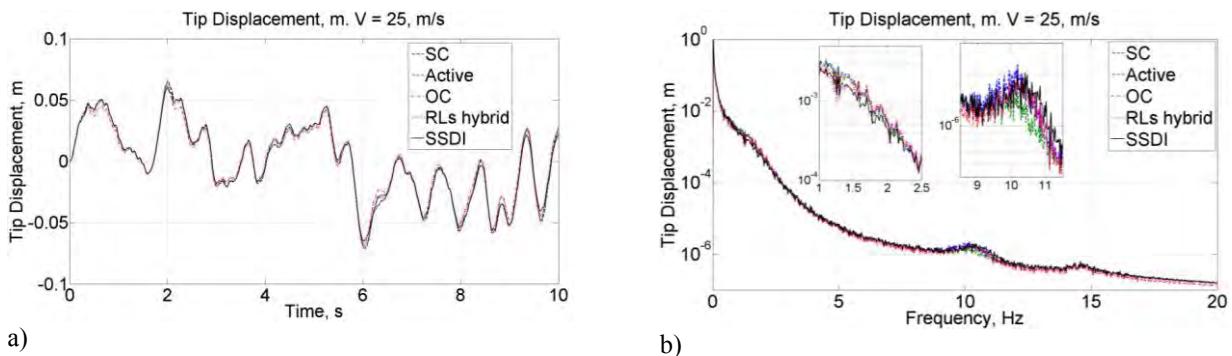
Figure 15: a) Piezoaeroelastic response to an atmospheric turbulence in time domain. b) Piezoaeroelastic response to an atmospheric turbulence in frequency domain

T.M.P. Silva and C. De Marqui Jr.
Multi-modal Piezoelectric Circuits for Vibration Suppression of a Plate-Like Wing Under Atmospheric Turbulence.
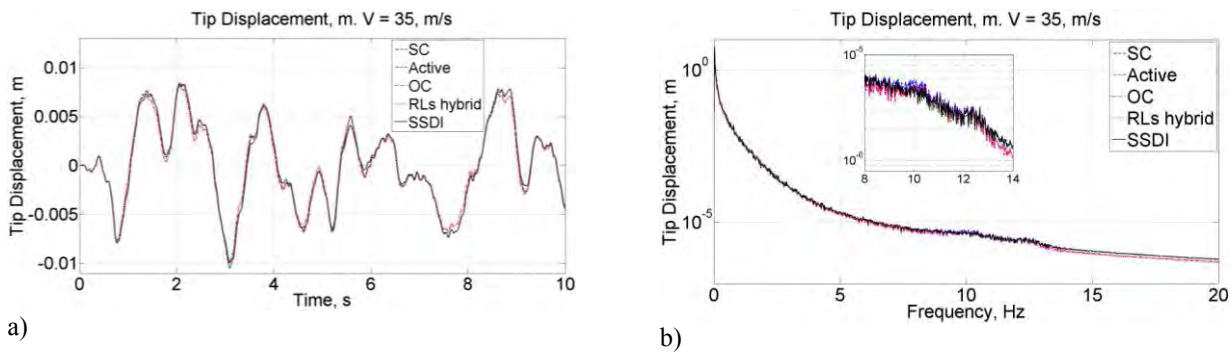
Figure 16: a) Piezoaeroelastic response to an atmospheric turbulence in time domain. b) Piezoaeroelastic response to an atmospheric turbulence in frequency domain.

At the flutter speed, the aerodynamic damping is zero and vibration attenuation is an important issue. Figures 17a and Fig. 17b show the piezoaeroelastic behavior under turbulence for the flutter speed in time and frequency domain.
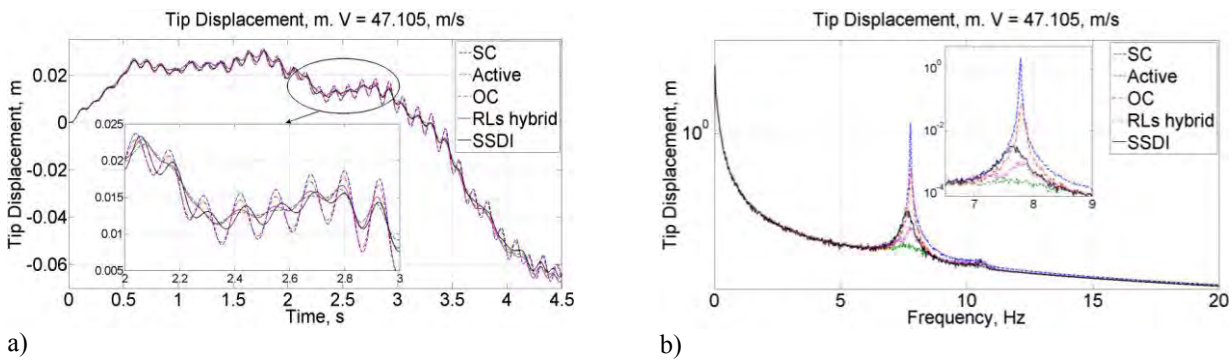
Figure 17: a) Piezoaeroelastic response to an atmospheric turbulence in time domain. b) Piezoaeroelastic response to an atmospheric turbulence in frequency domain

As seen in Fig. 17a, the presence of different piezoelectric circuits has negligible effect to reduce turbulence induced vibration at the flutter speed. The effect of the piezoelectric circuits is only visible at the enlarged view of Fig. 17a. As observed in the time history, crescent oscillations are observed for the SC case. In Fig. 17b, however, it is observed that the piezoelectric circuits efficiently reduced the flutter peak. In this case, the active and hybrid cases have better performance than the SSDI case. However, as the flutter frequency is poorly excited by the atmospheric turbulence, the reduction of its peak has little effect in time domain. As a bending-torsion mode is present at the flutter condition, cancelation of electrical output occurs. Therefore, considerable amount of energy is required to reduce the flutter peak as shown in Fig. 18a and Fig. 18b. As shown in Fig. 18a, the active and hybrid controller required similar amount of energy.
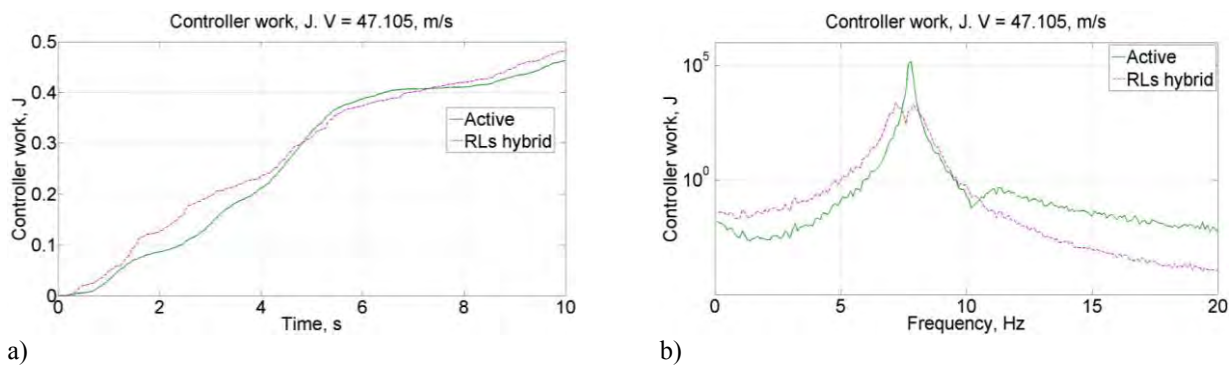
Figure 18: a) Energy required by the active and hybrid controller in time domain. b) Energy required by the active and hybrid controller in frequency domain

5. CONCLUSIONS

A novel atmospheric turbulence and flutter alleviation concept is investigated in this paper. The efficiency of different control schemes (passive and semi-passive circuits, an active controller and a hybrid network) for vibration reduction of an elastic wing with embedded piezoceramics is verified for several airflow speeds. The performance of the different piezoelectric circuits is more evident when the aerodynamic damping is low. Low aerodynamic damping is obtained at low airspeeds and close to the flutter speed. The hybrid controllers showed to be an interesting alternative to the purely active controller since less (or no) external energy is required. A similar performance (in terms of attenuation) was obtained for the SSDI and active cases. In addition, the hybrid and the active controllers could expand the flutter envelope while passive circuits have a poor performance in the post flutter condition. Although the oscillations are not damped out when the SSDI scheme is used at the airflow speed of 48m/s, the wing tip displacement is bounded and the wing presents acceptable mechanical amplitudes. It is important to remember that external energy is not required in the SSDI case, while power consumption of the active and hybrid cases is relatively large.

Atmospheric turbulence induced vibration by is discussed in the second case study. Atmospheric turbulence constitutes an important source of vibration for aircraft. The use of piezoceramics can provide significant attenuation when aerodynamic damping is negligible. For airflow speeds smaller than the flutter speed, the semi-passive circuit was as efficient as the hybrid controller.

6. ACKNOWLEDGMENTS

7. REFERENCES

Agneni A., Sorbo M. D., Mastroddi F. and Polli G. M., 2006. "Multi-modal damping by shunted piezo-patches: Possible aeroelastic applications." International Journal of Applied Electromagnetics and Mechanics 24 (2006) 1–24.

Agneni, A., Mastroddi, F. and Polli, G.M. 2003. ''Shunted Piezoelectric Patches in Elastic and Aeroelastic Vibrations,'' Computers and Structures, 81:91_105.

Agnes, G. S., 1994. "Active/passive piezoelectric vibration suppression". Proc. SPIE, Smart Struct. Mater. 2193 24–34

Agnes, G. S., 1995. "Development of a modal model for simultaneous active and passive piezoelectric vibration suppression" J. Intell. Mater. Syst. Struct. 6 482–7

Albano, E., and Rodden, W. P., 1969, "A Doublet-Lattice Method for Calculating Lift Distributions on Oscillating Surfaces in Subsonic Flow," AIAA J., 7, pp. 279–285.

Albano,E., Roddden,W.P. , "A doublet lattice method for Calculating lift distributions on oscillating surfazes in Subsonic flows", AIAA Journal, Vol. 7, No.2, February ,1969.

Anton, S. R., and Sodano, H. A., 2007, "A Review of Power Harvesting Using Piezoelectric Materials (2003–2006)," Smart Mater. Struct., 16, pp. R1–R21.

Blair, M., 1991, "A compilation of the mathematics method leading to the Doublet Lattice Method".

Cook-Chennault, K. A., Thambi, N. and Sastry, A. M., 2008, "Powering MEMS portable devices – a review of non-regenerative and regenerative power supply systems with emphasis on piezoelectric energy harvesting systems", Smart Materials and Structures 17 043001.

De Marqui Junior, C., Erturk, A. and Inman, D.J., 2009, "An electromechanical finite element model for piezoelectric energy harvester plates," Journal of Sound and Vibration, doi: 10.1016/j.jsv.2009.05.015.

De Marqui, Jr., C., Erturk, A., and Inman, D.J. 2009 "Piezo-Aero-Elastically Coupled Modeling and Analysis of Electrical Power Generation and Shunt Damping for a Cantilever Plate", Proceedings of the 17th International Conference on Composite Materials, Edinburgh, UK, 27-31 July 2009.

De Marqui, Jr., C., Erturk, A., and Inman, D.J. 2010, "Piezoaeroelastic Modeling and Analysis of a Generator Wing with Continuous and Segmented Electrodes". Journal of Intelligent Material Systems and Structures 2010 21: 983

duToit, N.E., Wardle, B.L. and Kim, S.–G., 2005, "Design considerations for MEMS-scale piezoelectric mechanical vibration energy harvesters," Integrated Ferroelectrics, 71, pp.21-160.

Erturk, A. and Inman, D. J., 2009. "Issues in Mathematical Modeling of Piezoelectric Energy Harvesters Smart Materials and Structures". Smart Materials and Structures, 17 065016

Erturk, A. and Inman, D.J., 2008, "A distributed parameter electromechanical model for cantilevered piezoelectric energy harvesters," ASME Journal of Vibration and Acoustics, 130, 041002.

Erturk, A. and Inman, D.J., 2009, "An experimentally validated bimorph cantilever model for piezoelectric energy harvesting from base excitations," Smart Materials and Structures, 18, 025009.

Erturk, A., Tarazaga, P., Farmer, J.R. and Inman, D.J., 2008, "Effect of strain nodes and electrode configuration on piezoelectric energy harvesting from cantilevered beams", ASME Journal of Vibration and Acoustics, 131, 011010.

Forward R. L., 1979. "Electronic damping of vibrations in optical structures". J. Appl. Opt. 18 690–7

Hagood, N. W. e von Flotow, A., 1991, "Damping of Structural Vibrations with Piezoelectric Materials and Passive Electrical Networks", Journal of Sound and Vibration, Vol. 146, Nº2, pp 243-268.

Johnson, C. D., 1995, "Design of Passive Damping Systems", Journal of Vibration and Acoustics Vol. 117, Special 50th Anniversary Design Issue, pp 171-176.

Kahn, S. P. and Wang, K. W., 1994. "Structural vibration controls via piezoelectric materials with active–passive hybrid networks". Proc. ASME IMECE DE75 187–94

Karpel, M. 1981. "Design for Active and Passive Flutter Suppression and Gust Alleviation" NASA Contractor Report 3482

Lazarus, K. B., Crawley, E. F., and Lin, C. Y., 1997, "Multivariable Active Lifting Surface Control Using Strain Actuation: Analytical and Experimental Results," J. Aircr., 34_3_, pp. 313–321.

McLean, D., 1969, "Automatic Flight Control Systems", Prentice Hall; 1 edition.pp 502.

Mohammadi S., 2008, "Semi-Passive vibration control using shunted piezoelectric material", PhD thesis, INSA.

Priya, S., 2007, "Advances in energy harvesting using low profile piezoelectric transducers" Journal of Electroceramics 19 167–184.

Roger, K.L., 1977. "Airplane Math Modeling Methods for Active Control Design,'! AGARD-CP-228.

S., Behens, S.O.R Moheimani and A.J. Fleming, 2003, Multiple mode current flowing passive piezoelectric shunt controller. Journal of sound and vibration, Vol. 266.

Sodano, H. A., Park, G., and Inman, D. J., 2004, "Estimation of ElectricCharge Output for Piezoelectric Energy Harvesting," Strain, 40, pp. 49–58.

Tsai, M. S. and Wang, K. W., 1999, "On the structural damping characteristics of active piezoelectric actuators with passive shunt," Journal of Sound and Vibration 221, 1–22.

Tsai, M. S. and Wang, K. W., 1999. "On the structural damping characteristics of active piezoelectric actuators with passive shunt," Journal of Sound and Vibration 221, 1–22.

Uchino, K. and T. Ishii, "Mechanical Damper Using Piezoelectric Ceramics," J. Jpn. Ceram. Soc. 96 (8), 863-867 (1988)

Wang S. T. and Frost W., 1980, Atmospheric turbulence simulation techniques with application to flight analysis. NASA contractor report 3309.

Wang, Y. and Inman, D.J, 2011, "Simultaneous Energy Haversting And Gust Aleviation For A Multifunctional Wing Spar Using Reduced Energy Control Laws Via Piezoceramics". SMASIS2011 – 5224.

Wu, S. Y., 1996. "Piezoelectric Shunts with Parallel R-L Circuit for Structural Damping and Vibration Control", Proc. SPIE Smart Structures and Materials, Passive Damping and Isolation; SPIE Vol. 2720, pp 259-269

Yuan, J., 2000, "Hybrid vibration absorption by zero/pole-assignment," Journal of Vibration and Acoustics 122, 466–469.

Zhao, Y., 2010, "Vibration Suppression of a Quadrilateral Plate Using Hybrid Piezoelectric Circuits", Journal of Vibration and Control, doi:10.1177/1077546309106529.

8. RESPONSIBILITY NOTICE

The authors are the only responsible for the printed material included in this paper.